



The multi-slice method for the design of a tubular linear motor with a skewed reaction rail

Benedikt Schmülling, Marc Leßmann, Björn Riemer and
Kay Hameyer

Institute of Electrical Machines, RWTH Aachen University, Aachen, Germany

Abstract

Purpose – A fundamental disadvantage of three-dimensional finite element (FE) simulations is high computational cost when compared to two-dimensional models. The purpose of this paper is to present an approach to minimize the computation time by achieving the same simulation accuracy.

Design/methodology/approach – The applied approach for avoiding high computational cost is the multi-slice method. This paper presents the adoption of this method to a tubular linear motor.

Findings – It is demonstrated that the multi-slice method is applicable for tubular linear motors. Furthermore, the number of slices and thereby computation time is minimized at the same accuracy of the simulation results.

Practical implications – The results of this paper offer a faster computation of skewed linear motors. At this juncture, the results are independent from the deployed FE solver.

Originality/value – The methods developed and proved permit a faster and more accurate design of tubular linear motors.

Keywords Simulation, Electric motors, Modelling, Computer aided design

Paper type Research paper

1. Introduction

Hydraulic and other mechanical damping systems are widespread in various industry applications. They feature a force increase depending on the displacement to their working point. This means that for conventional mechanic damping systems it is trouble to adjust the damping force to the optimum value, because they operate as simple proportional controllers. Furthermore, mechanic damping systems require much lubricant, e.g. hydraulic oil. Therefore, many dynamic oil seals are necessary, which are expensive, wear affected and often leaky. A good solution to prevent these disadvantages is the tubular synchronous linear motor presented in this work. It substitutes a hydraulic damper in combination with a spring. This spring-actuator system is controllable, adjustable, and oil-free. However, a disadvantage of this motor in its standard configuration is a very high force ripple due to the permanent magnets mounted to the reaction rail. This undesired effect has to be prevented. Therefore, a skewing of the magnets is considered. For the force computation of a tubular linear motor with skewed magnets, a three-dimensional finite element (FE) model is required, in principle. This model leads to very long modelling and computation times. To avoid this problem, the adoption of the so-called multi-slice method, which is verified for rotating machines (Schlensok *et al.*, 2006), is deployed. The multi-slice method combines several small FE-models of the actuator and yields results, which are in good



agreement to the output of the complete model simulation. The aim of this approach is the significant decrease of the entire computation time.

2. Constraints

The spring possesses a damping rate $k = 45 \text{ N/mm}$. The displacement x to the balanced point is at a maximum for $x_{max} = \pm 100 \text{ mm}$. The dimensions of the cylindrical installation space (shown in Figure 1) are: length $l = 400 \text{ mm}$, inner radius $r_{in} = 40 \text{ mm}$, and outer radius $r_{out} = 85 \text{ mm}$. The inner space of radius r_{in} comprises the spring in the centre of the installation space. Therefore, a tubular linear motor with a hollow reaction rail is recommended since this kind of actuator provides the maximum utilisation of space. A further advantage of tubular linear motors is the compensation of the normal forces to zero. Thus, the pressure on the bearings is very low and their estimated life cycle is high. The rated force of the motor shall be $F = 1,500 \text{ N}$ at a rated speed $v = \dot{x} = 1,200 \text{ mm/s}$.

1185

3. Analytical design

The analytical design process of the linear motor consists of the classical development steps for electrical machines. In a first step, the main dimensions of the motor are obtained. Furthermore, the detailed dimensioning is performed by the method of magnetic circuits. Finally, the winding design is performed.

3.1 Main dimensions

To avoid an energy supply to the moving part, a tubular linear motor with a stationary armature is chosen. For the displacement range, the rail has to stay within the limits of the armature yoke. Thereby, the edge effects, such as axial Maxwell forces are reduced. Hence, at an armature length of $l = 400 \text{ mm}$, the reasonable length of the reaction rail is $l_R = l - 2 \cdot |x_{max}| = 200 \text{ mm}$. The analytical part of the designing process contains the determination of the main reaction rail dimensions. With the aid of thrust σ , the diameter D of the reaction rail is calculated:

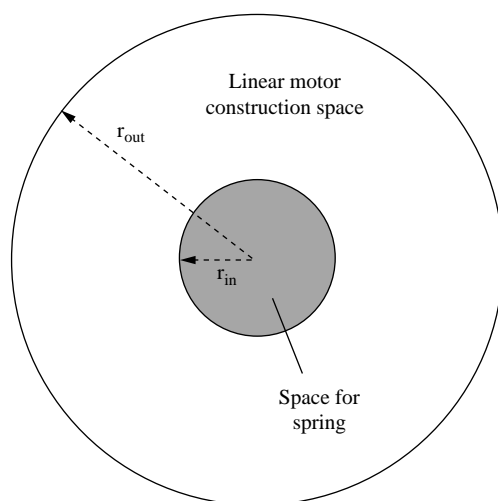


Figure 1.
Cross-section of the linear
motor construction space

$$\sigma = \frac{F}{A}. \quad (1)$$

Here, F is the force in moving direction and A is the surface area of the reaction rail. It is calculated as follows:

$$A = 2 \cdot \pi \cdot r_R \cdot l_R. \quad (2)$$

r_R is the outer radius of the reaction rail. Furthermore, the thrust is defined as:

$$\sigma = \frac{1}{2\pi} \int_0^{l_R} B(\alpha) \cdot A_{el}(\alpha) d\alpha. \quad (3)$$

B is the normal component of the air gap flux density and A_{el} is the electric load of the armature. In Müller *et al.* (2008), solutions of this equation can be found for standard rotational machines. These equations are adopted for the actual design process, since the method of operation is the same for rotational machines and linear motors. For a synchronous machine occurs:

$$\sigma_{sync} = \frac{\xi}{\sqrt{2}} \cdot \hat{B} \cdot A_{el} \cdot \cos(\Psi). \quad (4)$$

Literature (Müller *et al.*, 2008) specifies typical values for the required machine parameters. These parameters are used for a first analytical design step. The peak flux density \hat{B} , electric load A_{el} , load angle Ψ , and winding factor i are assumed to possess the following values:

$$\begin{aligned} \hat{B} &= 1 \text{ T} \\ A_{el} &= 40 \text{ kA/m} \\ \Psi &= 0^\circ \\ \xi &= 0.95. \end{aligned} \quad (5)$$

Merging equations (1), (4), and (5) and solving the equation for the outer radius of the reaction rail yields:

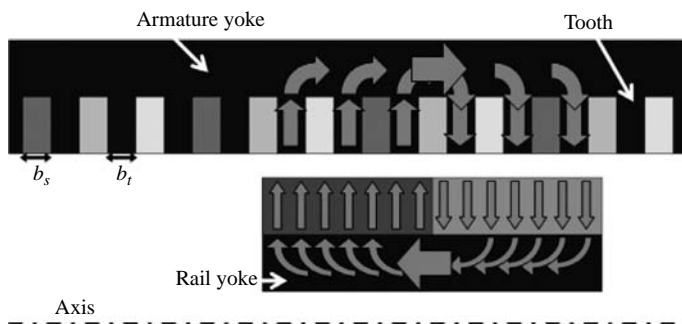
$$r_R = \frac{F}{\sqrt{2} \cdot \pi \cdot l_R \cdot \xi \cdot A_{el} \cdot \hat{B}}. \quad (6)$$

Solving this equation for $F = 1,500 \text{ N}$ yields the minimum radius, which is necessary to provide the required force.

3.2 Magnetic circuit

The detailed dimensioning of the active parts of reaction rail and armature is performed by the calculation of the magnetic circuit. A symbolic cross-section of the damper is shown in Figure 2. Armature teeth, armature yoke, rail yoke and permanent magnet height have to be designed. The limiting parameter is the saturation flux density of iron $B_{sat} = 1.8 \text{ T}$. A standard three-phase system is chosen and the pole number p is ascertained. A high-pole number is preferable, due to the possible reduction of yoke height in armature and reaction rail. However, the pole number is

Figure 2.
Symbolic cross-section of
reaction rail and armature



limited by the tooth width b_t , which decreases inversely proportional with the number of poles. b_t must not be arbitrary small, since then its mechanical stress exceeds the limitations. Subject to these limitations, the pole number is set to $p = 8$. Hereby, the number of teeth is known and tooth width b_t and slot width b_s are calculated. The dimensions of reaction rail yoke and armature yoke are also limited by the saturation flux density B_{sat} and they are determined similarly.

3.3 Winding design

The winding design depends on the terminal voltage U_T , which is the limitation value for the electromotive force U_{ind} . The number of turns per coil w is determined to utilise the terminal voltage with a high efficiency.

4. Computation without skewing

To verify the analytical design, a three-dimensional FE-computation is performed. For reducing the computation time, the model of the motor is limited to a 30° part of the complete motor due to symmetry according to the unskewed design. The model is shown in Figure 3. The boundary conditions of the sectioned areas are assumed as Dirichlet boundary conditions since the flux is directed to radial or axial direction.

The results are in good agreement with analytical calculations. The difference between the average forces of analytical design and FE-method amounts to less than 7 per cent. However, the force ripple is at a peak-to-peak value $\Delta F_r \approx 2,000$ N at rated operation not acceptable. The value of the cogging forces ΔF_c in open-circuit operation amounts nearly the same. To compensate the cogging forces, a skewing of both reaction rail magnets and armature teeth is possible.

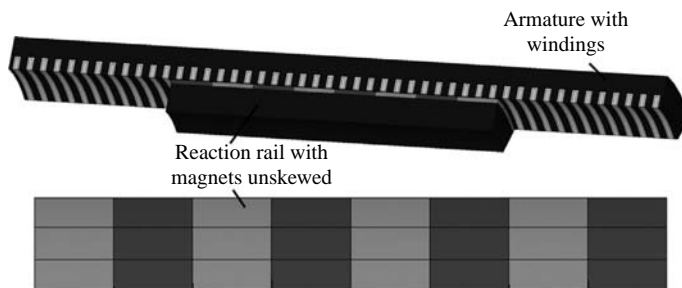


Figure 3.
 30° FE-model of the linear
motor unskewed

5. Half model of the skewed motor

To compensate the cogging forces, a skewing of the permanent magnets on the reaction rail is proposed. The benefit of this method compared to the method of the skewed armature teeth is the easier construction. Here, it is necessary to skew the magnets about one tooth distance over a length of half a rotation. An illustration of this skewing is shown in Figure 4. The displayed positions of the reaction rail's magnets relating to the armature teeth show the principle of operation. The integral cogging force is compensated by itself at any displacement. In contrast to rotational motors, the skewing is established in axial and not in transverse direction.

To compute this skewed layout, a 30° model of the motor is inadequately. Therefore, at least, a 180° model of the motor is required. This model is shown in Figure 5. It can be seen that the entire length of the reaction rail is increased about one tooth distance due to the skewing. Thereby, the maximum displacement is reduced by about 4 mm. Compared to simulations performed with the 30° model, the computation time increases considerably. All results presented are relating to a 360° model. At first, the pure cogging

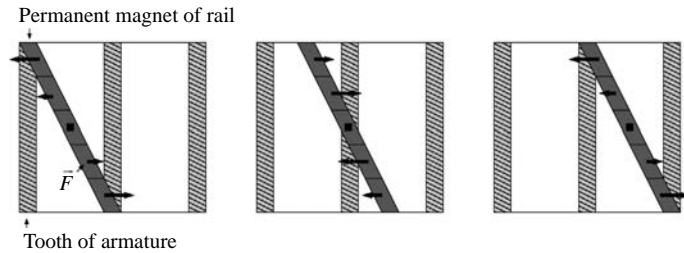


Figure 4.
Schematic skewing
illustration

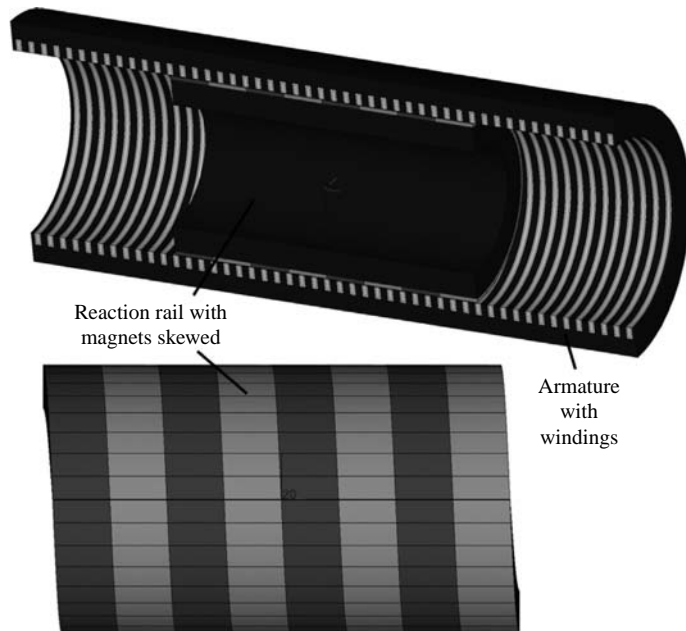


Figure 5.
180° FE-model of the
linear motor skewed

force is examined. Therefore, a computation in open-circuit operation is performed. No cogging force may be expected due to the skewing. However, the results presented in Figure 6 show a resulting force. This force is caused by leakage effects at the end sections of the reaction rail disregarded in the analytical design process. The peak-to-peak value of the cogging force in open-circuit operation results in $\Delta F_c \approx 40$ N.

To investigate the effects of skewing to the integral force, a computation of the rated operation is performed. The results presented in Figure 7 show an average force $F \approx 1,370$ N and a reduced force ripple $\Delta F_r \approx 90$ N. For this reason, the skewing of the reaction rail succeeds. The disadvantage of this procedure is the high computational cost to achieve the results. The computation time elapsing amounts to more than 5 h for each computation step. For an optimisation process, which requires the evaluation of several model variations, this continuance is not acceptable.

6. Multi-slice method

A time-optimised approach to compute skewed motors is the multi-slice method, which is well known for rotational machines (Schlensok *et al.*, 2006). Here, the motor model is composed of several slices of the whole motor. In principle, this method is a discretisation of the continuous skewing. The more slices the model contains, the more detailed is the discretisation. Owing to each slice is only a separate part of the 180° model, computation is parallelised and computation time is reduced by far. A reasonable superposition of the computation steps leads to the results requested. The application of this method to the linear motor described above is established similarly.

6.1 Twenty displaced 9° models

A first approach is the deployment of 9° models. Therefore, 20 models are created, which are displaced about a 20th slot pitch. Figure 8 shows a schematic description of

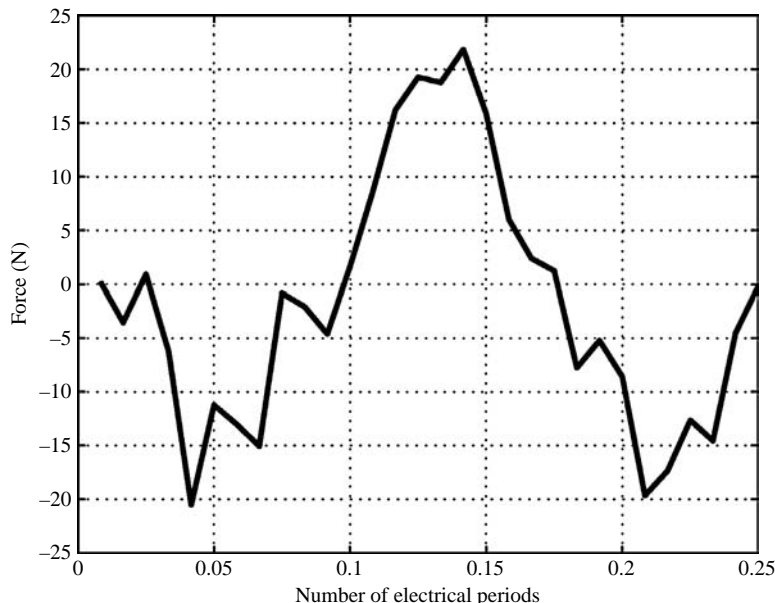


Figure 6.
Cogging force simulation
of the skewed 180° model

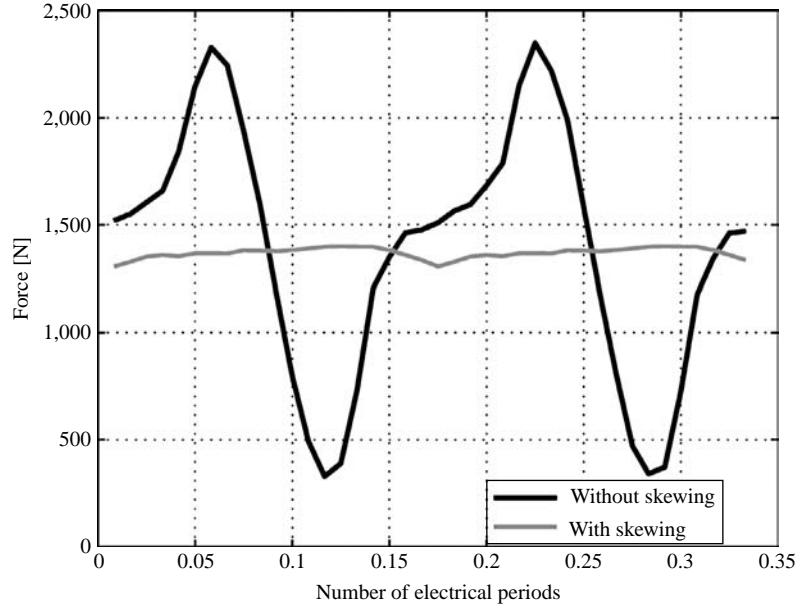


Figure 7.
Force simulations
of the 180° model

Note: Unskewed and skewed

the 9° models representing a section of the linear motor. The specific models can be seen on the y -axis. The skewing of the magnets complies with a 20th slot pitch. For illustration, the length of the magnet is reduced to one slot pitch. The computation is performed with the transient solver iMOOSE.tsa3d, an extension of the solver environment iMOOSE (van Riesen *et al.*, 2004), akin to the calculation of the 180° model. The current feed of each model is the same. The resulting force of each computation step occurs by addition of the individual results:

$$F = \sum_{m=1}^{20} f_m. \quad (7)$$

Here, m is the model number and f_m is the time-dependent force of every slice. The results of this computation method are in good accordance with the results of the 180° model. The average propulsion force amounts to $F = 1,370$ N. The deviations are within a range of ± 40 N, which are based on differences in discretisation.

The computational cost of this simulation amounts to 2 h for 40 time steps of one model. This means, the entire computation time is reduced by factor 10 compared to the computation of the 180° model. A further benefit is the possibility to parallelise the simulation of each model, which additionally yields a reduction of factor 20 in computation time.

6.2 Reduction to one 9° model

A further approach is the opportunity to minimise the number of necessary computations. Taking the symmetry of the different slices into account, only one slice is required to compute the entire motor.

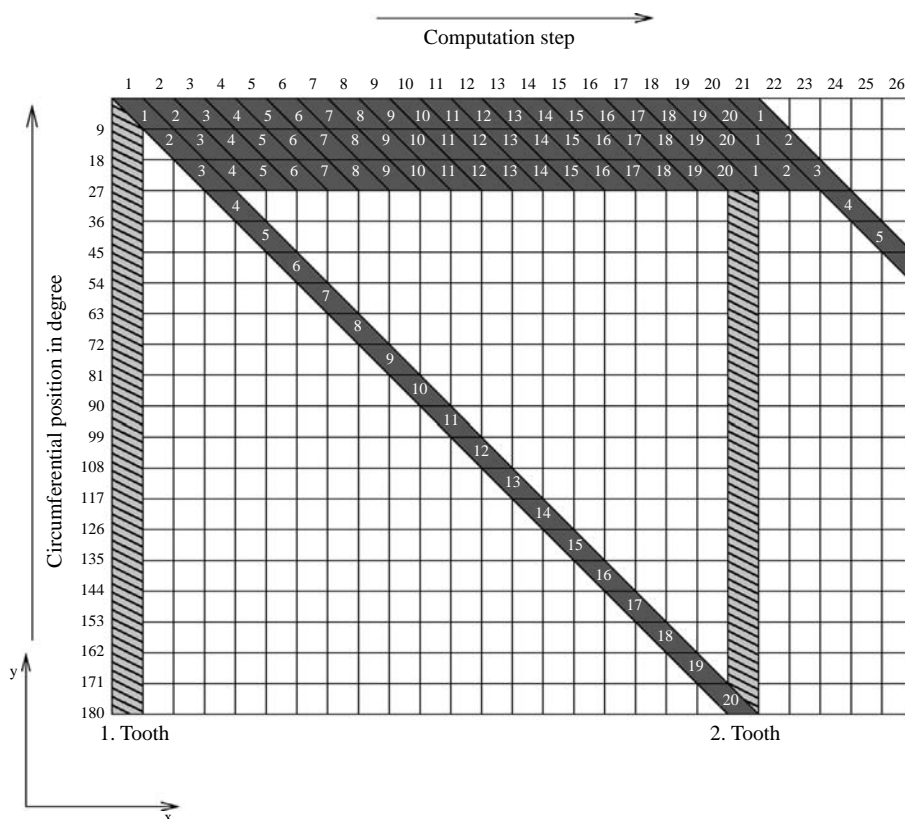


Figure 8.
Arrangement of the
20 skewed 9° models

In the following, only the first 9° model is used. By utilisation of the symmetry, all other models can be displayed by the first one. Cause for this purpose is the use of a model angle of 9°, which is a 20th part of the 180° model, and the fact that one electrical period is split in 20 discrete computation time steps. In Figure 8, it can be seen that the second computation step of the first model equals to the first computation step of the second model. Therefore, it is possible to calculate the entire computation step of the 180° model by addition of the first 20 steps of the first 9° model. For the second computation step, the steps 2 until 21 of the 9° model are accumulated. All further time steps are calculated as follows:

$$F_{i=1..20} = \sum_{j=i}^{i+19} f_j. \quad (8)$$

i is the step number of the 180° model and j is the number of the transient time step of the 9° model.

To calculate the first 20 time steps of the entire motor, 40 time steps of the reduced model are required. The difference of this results compared to the results of the computation method with 20 models is less than 0.5 N. The entire computational time compared to the former method is reduced by factor 1/10.

6.3 Skewing discretisation

A final simplification of the computation procedure is the buildup of the 9° model with unskewed magnets. Figure 9 shows the arrangement of 20 models forming the entire linear motor similar to Figure 8. It can be seen that the skewing of the magnets is discretised. This is a preliminary stage of a two-dimensional computation of the linear motor, due to the symmetry of one model. For this, an axial symmetric transient solver is required. The propulsion force is calculated in the same way as described in the former section.

6.4 Synopsis

The results of the FE-computation using the multi-slice method show a very good accordance with the results of one 180° simulation. Here, the computation of one step lasts only a few minutes. Figure 10 shows the comparison of all computation results. It can be seen that the results of the three simplified methods are nearly the same. The deviation to the results of the full model are higher but also insignificant. Table I shows the computational costs of the four computation methods. The simulation of the 180° model requires more than 20 days to be performed. By application of the multi-slice method, this computation can be reduced to a duration of 6 h.

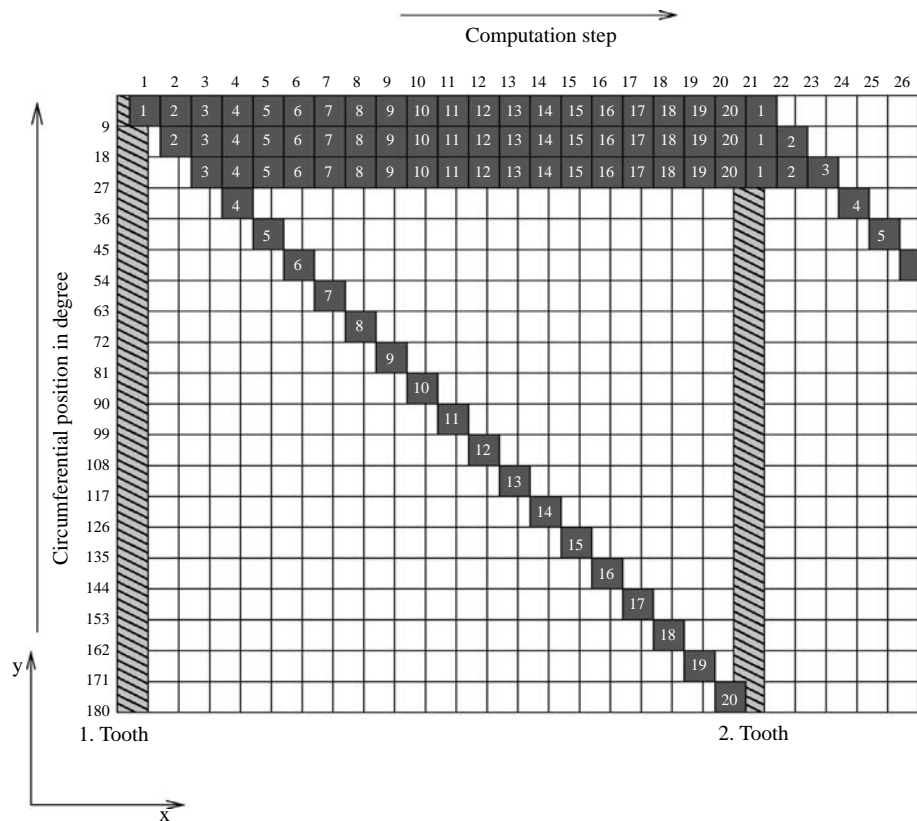


Figure 9.
Arrangement of the
20 unskewed 9° models

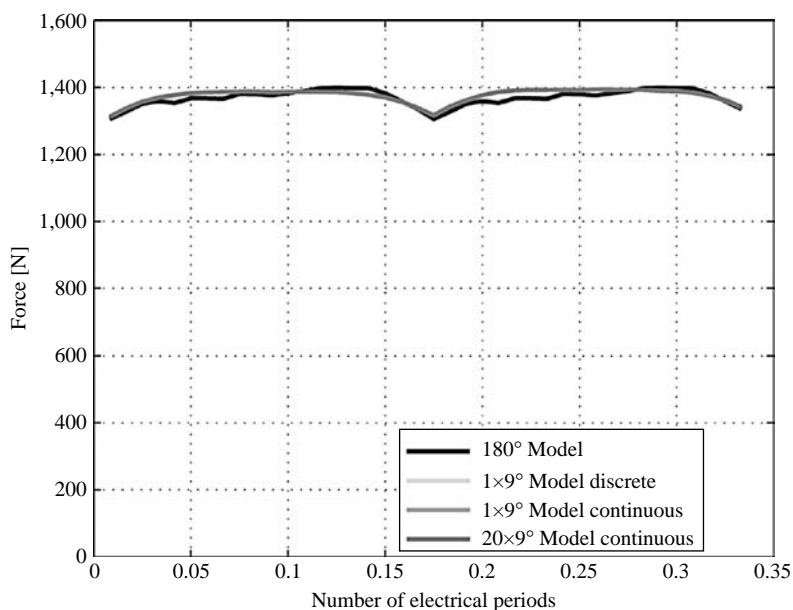


Figure 10.
Comparison of all force
computation methods

Model	Computational cost
180° model	> 20 days
Twenty 9° models	45 h
One 9° model	6 h
One 9° model with discretised skewing	6 h

Table I.
Comparison of the entire
computation time

The great benefit of the last method is the possibility to perform the computation with one two-dimensional model. If this would be applied, the computation time will be reduced farther.

7. Conclusion

The analytical design of a tubular linear motor is presented. An evaluation of the motor layout by FE-simulation showing the unacceptable force ripple is performed. To optimise the layout, a skewing of the reaction rail is proposed. Further simulations show that the evaluation method using a 180° model of the motor is not feasible. Therefore, the multi-slice method, which allows the avoiding of full models for skewed rotors, is used to compute several working points of the motor. For this, 20 displaced 9° models of the linear motor are deployed. By using this method in conjunction with parallel computation, the computation time is decreased from about one day per time step down to a few minutes. Here, the application of this method shows nearly the same results as the 180° FE-simulation pre-mentioned. Two further simplifications of the multi-slice method, the deployment of only one 9° model, once skewed and once unskewed, yields nearly the same results as the other method. Hereby, the computation time is reduced to 6 h all in all.

The adoption of the multi-slice method for the design of the tubular linear motor was successful, since the computation time is reduced by far and the results comply with each other.

References

- Müller, G., Vogt, K. and Ponick, B. (2008), *Berechnung elektrischer Maschinen*, Wiley-VCH Verlag GmbH & Co. KGaA, Weinheim.
- Schlensok, C., van Riesen, D., Seibert, D. and Hameyer, K. (2006), "Fast structure-dynamic simulation of electrical machines using 2D-3D-coupling", paper presented at 6th International Conference on Computational Electromagnetics, CEM, Aachen.
- van Riesen, D., Monzel, C. and Kaehler, C. (2004), "iMOOSE – an open-source environment for finite-element calculations", *IEEE Transactions on Magnetics*, Vol. 40 No. 2, pp. 1390-3.

About the authors

Benedikt Schmülling was born in Herne/Westphalia, Germany, on 8 March 1980. He received his MSc degree in Electrical Engineering in 2005 from the University of Dortmund and his PhD degree in 2009 from RWTH Aachen University. Since 2005, he has worked as a Researcher at the Institute of Electrical Machines (IEM). He has worked on machine acoustics, linear motor technology and magnetic levitation systems. He is a member of VDI and VDE. Benedikt Schmülling is the corresponding author and can be contacted at: Benedikt.Schmuelling@iem.rwth-Aachen.de

Marc Leßmann was born in Arnsberg, Germany, on 14 November 1977. He received his MSc degree in Electrical Engineering in 2004 from RWTH Aachen University. Since 2004, he has worked as a Researcher at the IEM. He has worked on linear motors, magnetic levitation systems and high speed drives.

Björn Riemer was born in Viersen, Germany, on 16 March 1982. He received his MSc degree in Electrical Engineering in 2009 from RWTH Aachen University. Since 2009, he has been a Researcher at the IEM. His research interests include electromagnetic field calculation as well as simulation and design of electrical machines.

Kay Hameyer was born in Hannover, Germany, on 20 June 1958. He received his MSc degree in Electrical Engineering from the University of Hannover and his PhD degree from the Berlin University of Technology. After his university studies, he worked with the Robert Bosch GmbH in Stuttgart as a Design Engineer for permanent magnet servo motors and board net components. Until 2004, Professor Kay Hameyer was a full Professor for Numerical Field Computations and Electrical Machines with the KU Leuven in Belgium. Currently, he is the Director of the IEM and holder of the Chair Electromagnetic Energy Conversion of the RWTH Aachen University in Germany. He is a senior member of VDE and IEEE.